

Bacillus subtilis Assisted Assembly of Gold Nanoparticles into Long Conductive Nodous Ribbons

Yonghong He,[†] Jinying Yuan,^{*,†} Fengyi Su,[‡] Xinhui Xing,[‡] and Gaoquan Shi^{*,†}

Key Lab of Organic Optoelectronics & Molecular Engineering of Ministry of Education, Department of Chemistry, Tsinghua University, Beijing 100084, People's Republic of China, Department of Chemical Engineering, Tsinghua University, Beijing 100084, People's Republic of China

Received: June 15, 2006; In Final Form: July 14, 2006

Gold nanoparticles with diameters of about 20 nm were assembled onto the surfaces of *Bacillus subtilis* by keeping the mixture of the nanoparticles and the bacteria in the dark without disturbance for over a month. During the aging process, the bacteria connected to each other end-to-end to form long wires and gold nanoparticles were coated compactly onto the surfaces of the wires simultaneously. The resulting composite wires were collapsed into ribbons with a width of about 1 μm after drying in air. The ribbons present a novel structure with nodes on their backbones and have lengths of several millimeters. They are conductive and showed Ohmic behavior, which provides potential applications in the fabrication of electronic nanodevices.

Introduction

Gold nanoparticles have received great interest owing to their unique optical and electronic properties.^{1–4} For the fabrication of nanodevices and with the objective of reuse while retaining their properties, gold nanoparticles are usually required to be assembled to micro-sized or larger architectures.^{5–8} Extensive work also has been devoted to the assembly of Au nanocrystals into spheres,⁹ rods,¹⁰ or wires,¹¹ and tubes.¹² Organic reagents such as benzene and anthracene¹³ and toluene¹⁴ can assist the assembly of Au nanoparticles in aqueous solutions. The organization of gold nanocrystals at the liquid–liquid interface can be achieved via cation– π interaction between the aromatic molecules and nanoparticle surface-bound Au^+ ions.¹⁴ Inorganic reagents such as NaOH and NaCl were also used to assist the formation of silver wires.^{15,16} However, successful fabrication of ordered nanoparticle aggregates in solutions usually needs a template such as DNA,¹⁷ virus,¹⁸ fungi,¹⁹ or polymers.^{20,21} Recently, Saraf and co-workers also reported the methods of assembling gold nanorods on individual live bacterium to obtain highly conductive hybrid system²² or to fabricate electronic devices.²³ In this paper, we desire to report a *Bacillus subtilis* assisted assembly of gold nanoparticles into nodous ribbons. The end-to-end connection of live bacteria provided a long template for assembling the nanoparticles, which resulted in the formation of ribbons with a length of several millimeters. More interestingly, there are regular nodes on the backbones of the ribbons, which gave them a bamboo-like structure.

Experimental Section

Growth of *Bacillus subtilis*. *Bacillus subtilis* 168, grown on nutrient agar plates, were inoculated in nutrient broth (8 g/L Tryptone, 5 g/L Yeast extract, 10 g/L NaCl) and incubated in a shake flask at 37 °C for 24 h. Then, the bacteria were washed three times by centrifugation at 4000 rpm for 15 min each, and

finally suspended in a phosphorus buffer solution (135 mM NaCl, 3 mM KCl, 10 mM Na_2HPO_4 , 2 mM KH_2PO_4 and adjusted with HCl to pH 7.4) at 4 °C for further use.

Synthesis and Assembly of Gold Nanoparticles. The gold nanoparticles (~ 20 nm) used in these findings were synthesized by the well-known citrate reducing method.²⁴ Briefly, 15 mL of a 0.001 M aqueous solution of HAuCl_4 (Beijing Jingyi Chem. Co., Analytical Grade) was boiled for 15 min under vigorous stirring. Then, 15 mL of a 0.01 M aqueous solution of tripotassium citrate (Beijing Jingyi Chem. Co., Analytical Grade) was added to reduce HAuCl_4 into gold nanoparticles, which resulted in an indicative color change from purple red to red. The reaction was continued for another 15 min, and finally the solution was cooled to room temperature for use.

A phosphorus buffer solution (2 mL) of 10^6 CFU (Colony Forming Unit)/mL of *Bacillus subtilis* 168 was mixed with a 18 mL solution of gold nanoparticles described above. The content of gold nanoparticles in this system was calculated to be about 56 $\mu\text{g/mL}$. Then, the mixture was placed in the dark at 4 °C for more than 40 days without disturbance. During this period, a sample was taken from the mixture once a day for 7 days for SEM detection and tracking the activity of the bacteria by heterotrophic plate count (HPC) tests.

Instruments. The transmission and scanning electron micrographs (TEM and SEM) were taken with a JEOL JEM-1200 EX transmission electron microscope operated at an accelerating voltage of 120 kV and JEOL-JSM-6460LV field-emission scanning electron microscope operated at an accelerating voltage of 10 kV, respectively. The energy-dispersive X-ray spectral (EDX) analysis was also carried out on the TEM instrument described above. X-ray photoelectron spectra (XPS) were recorded with use of a PHI-5300 ESCA X-ray photoelectron spectrometer at a pressure of 1×10^{-10} Torr. The core level spectra were background corrected by using the Shirley algorithm and the chemically distinct species resolved through a nonlinear least-squares procedure. Infrared spectra were recorded on a Nicolet 710 FT-infrared spectrometer. The current–voltage measurements were measured on an M 273 potentiostat–galvanostat (EG&G Princeton Applied Research)

* To whom correspondence should be addressed. Phone: +86-10-62773743. Fax: +86-10-62771149. E-mail: gshi@tsinghua.edu.cn. E-mail: yuanjy@tsinghua.edu.cn.

[†] Department of Chemistry.

[‡] Department of Chemical Engineering.

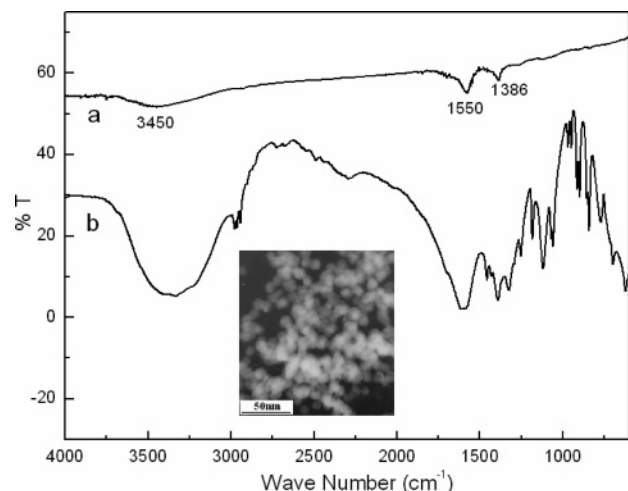


Figure 1. Infrared spectra of as-synthesized Au nanoparticles (a) and tripotassium citrate (b). Inset: A transmission electron micrograph of Au nanoparticles.

under computer control. The gold nanoparticle coated bacteria (AuNPCB) ribbons were deposited on a glass sheet and shaped into a $0.5 \times 6 \text{ mm}^2$ strip with a knife, and two copper electrodes were attached to the stripe with carbon conductive gel. The distance between the two electrodes was measured to be 2 mm.

Results and Discussion

Assembly of Gold Nanoparticles onto the Surfaces of *Bacillus subtilis*. Figure 1a is an infrared spectrum of the gold nanoparticles. This spectrum shows two absorption peaks at 1550 and 1386 cm^{-1} , indicating that there exist carboxylic groups bound to the gold nanoparticles. This is mainly due to citrate acting as both a reducing agent in the reaction and a capping agent for Au nanoparticles. A broad and strong peak centered at 3450 cm^{-1} in the spectrum of tripotassium citrate (Figure 1b) was greatly weakened in the spectrum of Au nanoparticles, indicating that the hydroxyl groups of the salt were partly oxidized to carbonyl groups. Thus, in aqueous solution, the surfaces of gold nanoparticles bring negative charges.²⁰ The TEM image of the gold nanoparticles shown as

the inset of Figure 1 indicates that the nanoparticles are round and have diameters of around 20 nm.

The mixture of gold nanoparticles and bacteria exhibits the characteristic intense red color of Au nanoparticles. During the process of aging in the dark, the Au nanoparticles in the solution gradually assembled onto the surfaces of the bacteria. This led to the formation of a reddish purple macroscopic material that phase separated from the aqueous medium. As a result, the color of the mixture also gradually changed to transparent. Figure 2a represents the image of freshly obtained *Bacillus subtilis*, which have a diameter of ca. 0.8 μm and a length of ca. 2.0 μm . It is clear from this image that the bacteria were shriveled due to drying in air. In this stage, the bacteria are in discrete states. Figure 2b indicates that there are Au nanoparticles attached to the bacteria after aging for 1 day. The coverage ratio of Au nanoparticles on the bacterium increased with the increase of aging time and reached about 70% after 2 weeks (Figure 2c). Meanwhile, the bacteria were connected to each other end-to-end. Finally, the bodies of bacteria were compactly covered by Au nanoparticles after aging for 4 weeks (Figure 2d).

It is known that the surfaces of *Bacillus subtilis* bring negative charged teichoic acid brushes.^{22a} Thus, the surfaces of the bacteria and Au nanoparticles have the same charges and the electrostatic interaction was not the main driving force for assembling nanoparticles on the surfaces of the bacteria. On the other hand, as established by the theory of hard and soft acids and bases, noble metals such as silver or gold have the affinity to react with phosphorus and sulfur groups.^{25–27} The membranes of the bacteria are well-known to contain many sulfur-containing proteins²⁸ which can act as the sites for Au nanoparticle attachments. Furthermore, there are many active bacterial cells on the ends of each bacilliform bacterium, and many cells collect to form a group on the tip of each growing branch.^{29–32} *Bacillus subtilis* also can be connected into long wires through the active bacterial cells on their tips.^{30–32} In this study, we controlled the concentration of the nanoparticles (56 $\mu\text{g/mL}$) to be lower than the critical value (ca. 75 $\mu\text{g mL}^{-1}$) and kept the cells alive and growth in the initial 2 weeks of aging.³³ Thus, the bacteria connected to each other to form rod-shaped wires and gradually deposited onto the bottom of the

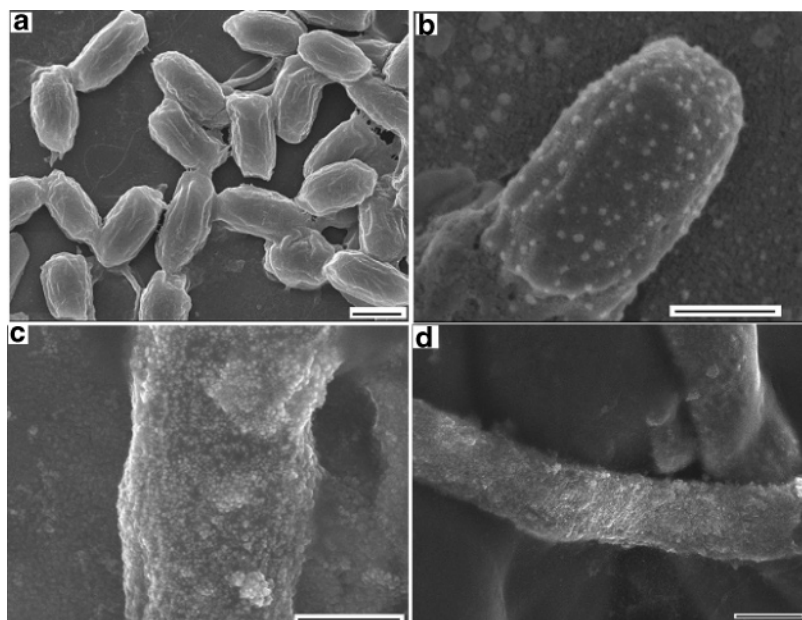


Figure 2. SEM images of freshly grown bacteria *Bacillus subtilis* (a) and the surface of a bacterium coated with Au nanoparticles formed by aging the mixture of Au nanoparticles and the bacteria for 1 day (b), 2 weeks (c), and 4 weeks (d), respectively. Scale bar: 1 μm .

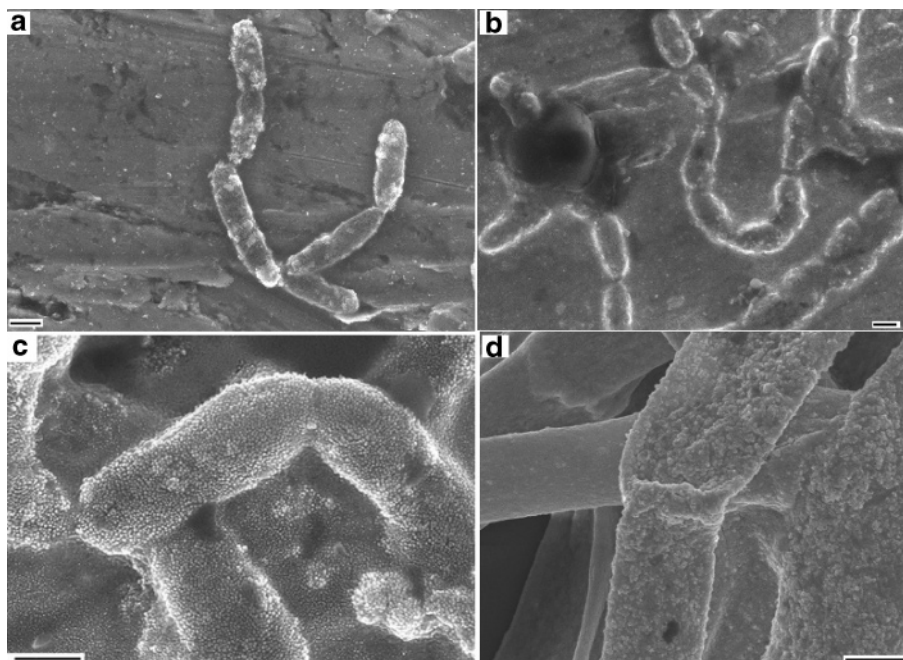


Figure 3. SEM images of the AuNP-CB wires formed by aging for 1 (a), 3 (b), 4 (c), and 6 week (s), respectively. Scale bar: 1 μm .

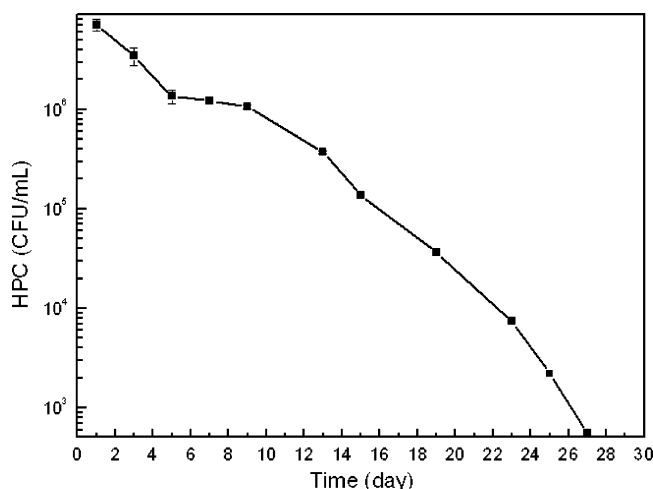


Figure 4. Plot of heterotrophic plate counts (HPC) versus aging time.

flask. Figure 3a shows that the bacteria start to connect to each other end-to-end based on the active bacterial cells at their tips after aging for 1 week. In the following 2 to 3 weeks, almost all the bacteria were connected together to form long wires (Figure 3b,c). It is clear from these figures that the bacterial wires were compactly covered with Au nanoparticles, even at the bacteria tips. More importantly, during the course, the bacteria tips produced more proteins with a sulfur group than those at their bodies. As a result, more Au nanoparticles were attached to the nodes of the bacteria wires than those on the bacteria bodies as shown in Figure 2d. This is why the resulting Au nanoparticle-coated bacteria (AuNP-CB) wires have uniform width, while the nodes can be distinguished from the microscopic images shown below. The Au nanoparticles at the bacterial tips also helped the directional assembly of Au nanoparticle-coated bacteria.

The HPC study results are plotted in Figure 4. This plot demonstrated that about 50% of the bacteria kept their activity and reproducibility in the initial two weeks of aging. This made the bacteria connect with each other into wires and produce proteins for the attachment of Au nanoparticles. With the

consuming of nutritive and the attachment of Au nanoparticles on their surfaces, the bacteria lose their activities quickly. After aging for 4 weeks, approximately 99.9% of the bacteria had died and could no longer produce proteins. The AuNP-CB wires precipitated to the bottom of the flask. Successively, free Au nanoparticles in the solution continued to coat the surfaces of these bacteria during the following period because of sedimentation.

As the bacteria were died, their bodies started to decompose. As a result, the size of a dead bacterium is smaller than that of a live one. Thus, the long composite wires were gradually shrunken and broken away from the "mother" Au nanoparticle film, leaving behind slots in the film. As shown in Figure 5a, a film of piled Au nanoparticles (bright regions) with slots (black regions) resulted from removing the AuNP-CB wires. The magnified image of the flat bright region indicates that the film is made up of Au nanoparticles (Figure 5b). When AuNP-CB nanowires were transferred to the surface of a glass sheet and dried in air, they collapsed to a belt-shaped structure (Figure 5c,d).

Figure 6a shows a mass overview of the resulting ribbons after washing with deionized water ($3\times$) and drying in air. The length of these ribbons can reach several millimeters. The magnified view proves that the ribbons are composed of a large number of Au nanoparticles (Figure 6b,c). The connected tips of the bacteria can be distinguished from the SEM image shown in Figure 6d, and the ribbons have a bamboo-like structure. Furthermore, the AuNP-CB ribbons exhibit a golden hue. The inset image in Figure 6d is an optical image recorded by the CCD camera of the Renishaw PLC Raman spectrometer; the nodes exhibit relatively dark color, while the uniform segments show the bright golden color of the Au nanoparticles.

Spectroscopic Characterizations and Electronic Property of the AuNP-CB Ribbons. The EDX spectrum shown in Figure 7 indicates that the ribbons are composed of 93.06 wt % gold and 1.83 wt % carbon. The gold component can be assigned to Au nanoparticles. The peaks at 2.1, 9.7, and 11.8 keV can be assigned to metallic gold, and the carbon peak was originated from the bacteria and the capping agents on the nanoparticle surfaces. Figure 8 illustrates the XPS spectrum of the Au ribbons

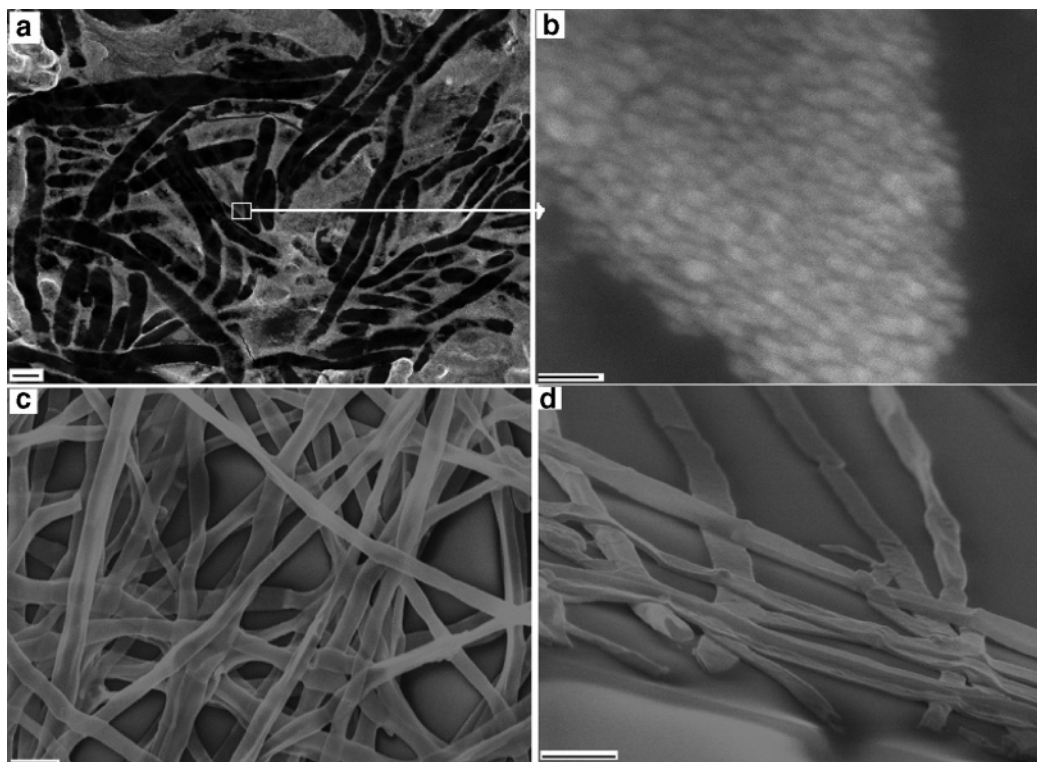


Figure 5. SEM images of a Au nanoparticle film with slots (black regions) after removing the AuNP-CB wires (a), a regional magnified view of the nanoparticle film (b), and AuNP-CB ribbons located on a glass sheet (c, d). Scale bars: 1 μm (a, c d) and 100 nm (b).

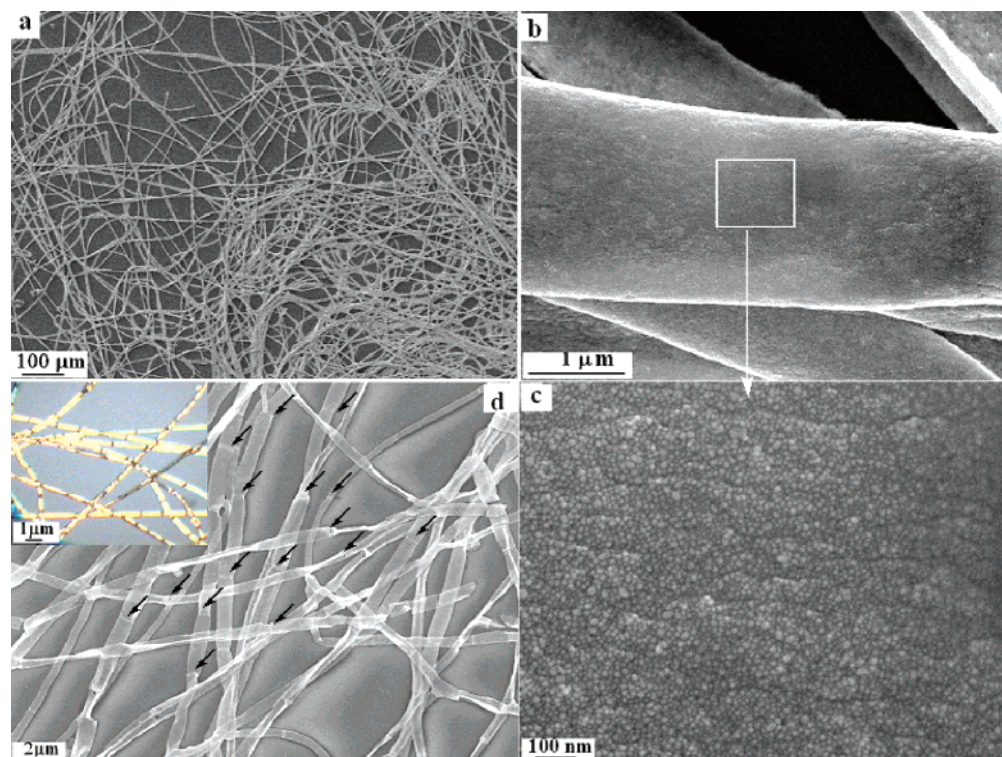


Figure 6. SEM images of an overview of mass AuNP-CB ribbons (a) and the magnified views of the ribbons (b–d). The arrows in panel d point to the nodes of the ribbons and the inset of panel d is an optical image of the AuNP-CB ribbons.

placed on the common thin glass sheet. The O (1s), Au (4f), Au (4d), Au (4p), and C (1s) signals show a typical spectrum of the citrate reducing Au nanoparticles. The doublet peaks of Au 4f_{7/2} (83.7 eV) and Au 4f_{5/2} (87.4 eV) (shown in the regional spectrum as the inset of Figure 8) are characteristic of Au⁰. The absence of a band at 84.7 eV for Au⁺ in the Au nanoparticles also confirms that the Au atoms in the ribbons are Au⁰.

The current (*I*)–voltage (*V*) curve of a strip of the AuNP-CB ribbon mat (shown in Figure 6) is illustrated in Figure 9. The width of the strip is 0.5 mm and the distance between the two electrodes is 2 mm. The *I*–*V* curve exhibits a Ohmic behavior and the resistance was calculated to be approximately $2 \times 10^7 \Omega$. Saraf et al. reported that the bacterium coated with submonolayered roundish Au nanoparticles was an insulator.^{22a}

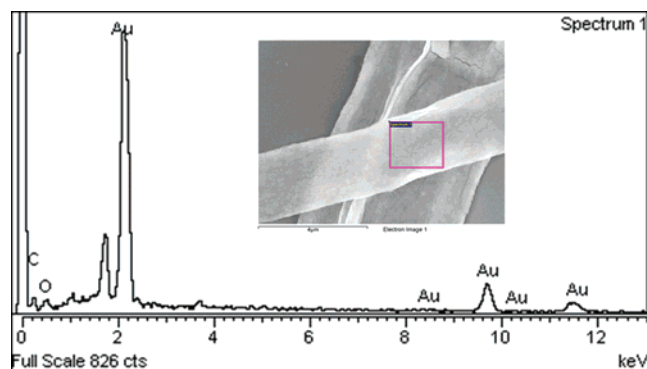


Figure 7. Energy-dispersive X-ray (EDX) spectrum of the AuNP-CB ribbon.

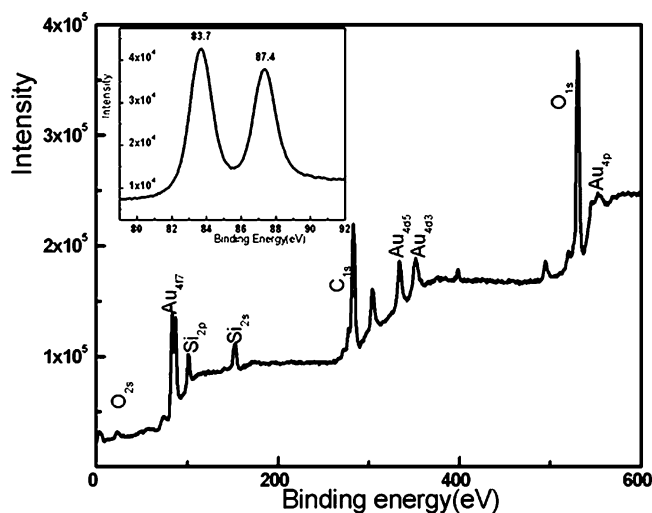


Figure 8. XPS spectra of the AuNP-CB ribbons.

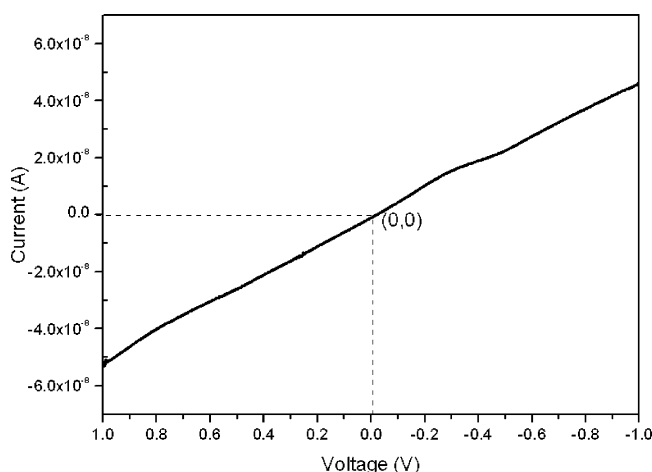


Figure 9. Plot of current (I) versus voltage (V) of the AuNP-CB ribbon mat (shown in Figure 6) with width of 0.5 mm and distance between the two electrodes of 2 mm.

However, in this case, the Au particles were assembled into compact ribbons with multilayered Au nanoparticles, which led the ribbons to be conductive.

Conclusions

This work provides a simple and economic example of how to use bacteria as the template to organize Au nanoparticles into long ribbons. In the process, *Bacillus subtilis* connected with each other via the cells on their tips to form long wires which served as the template for assembling Au nanoparticles.

The AuNP-CB ribbons formed by this technique exhibit a novel nodous structure. They have a width of ca. 1 μm and a length of several millimeters. The ribbons are conductive and show Ohmic behavior. The length and resistance of the ribbon may be controlled by the number of its nodous segments. Furthermore, the long ribbons can be interconnected into conductive networks. The large sizes of the ribbons and their networks makes them feasible to be tailored and applied in the fabrication of electronic nanodevices.

Acknowledgment. This work was supported by the National Natural Science Foundation of China (Nos. 20574042, 50373023, 50225311, 90401011, and 50533030).

References and Notes

- (1) Luedtke, W. D.; Landman, U. *Phys. Rev. Lett.* **1999**, *82*, 3835–3838.
- (2) Xiao, Y.; Patolsky, F.; Katz, E.; Hainfeld, J. F.; Willner, I. *Science* **2003**, *299*, 1877–1881.
- (3) Cui, X. D.; Primak, A.; Zarate, X.; Tomfohr, J.; Sankey, O. F.; Moore, A. L.; Moore, T. A.; Gust, D.; Nagahara, L. A.; Lindsay, S. M. *J. Phys. Chem. B* **2002**, *106*, 8609–8614.
- (4) Fu, Q.; Saltsburg, H.; Stephanopoulos, F. M. *Science* **2003**, *301*, 935–938.
- (5) Kim, S. W.; Kim, M.; Lee, W. Y.; Hyeon, T. *J. Am. Chem. Soc.* **2002**, *124*, 7642–7643.
- (6) Chen, C. W.; Chen, M. Q.; Serizawa, T.; Akashi, M. *Adv. Mater.* **1998**, *10*, 1122–1126.
- (7) Zheng, J. W.; Zhu, Z. H.; Chen, H. F.; Liu, Z. F. *Langmuir* **2000**, *16*, 4409–4412.
- (8) Chung, S. W.; Ginger, D. S.; Morales, M. W.; Zhang, Z. F.; Chandrasekhar, V.; Ratner, M. A.; Mirkin, C. A. *Small* **2005**, *1*, 64–69.
- (9) Bao, Z. N.; Chen, L.; Weldon, M.; Chandross, E.; Cherniavskaya, O.; Dai, Y.; Tok, J. B. H. *Chem. Mater.* **2002**, *14*, 24–26.
- (10) Jana, N. R.; Gearheart, L.; Murphy, C. J. *J. Phys. Chem. B* **2001**, *105*, 4065–4067.
- (11) Peng, X. G. *Adv. Mater.* **2003**, *15*, 459–463.
- (12) Oshima, Y.; Onga, A.; Takayanagi, K. *Phys. Rev. Lett.* **2003**, *91*, 205503-1–205503-4.
- (13) Kumar, A.; Mandal, S.; Mathew, S. P.; Selvakannan, P. R.; Mandale, A. B.; Chaudhari, R. V.; Sastry, M. *Langmuir* **2002**, *18*, 6478–6483.
- (14) Ramanath, G.; D'Arcy-Gall, J.; Maddanimath, T.; Ellis, A. V.; Ganesan, P. G.; Goswami, R.; Kumar, A.; Vijayamohan, K. *Langmuir* **2004**, *20*, 5583–5587.
- (15) Caswell, K. K.; Bender, C. M.; Murphy, C. J. *Nano Lett.* **2003**, *3*, 667–669.
- (16) Leontidis, E.; Kleitou, K.; Kyprianidou-Leodidou, T.; Bekiari, V.; Lianos, P. *Langmuir* **2002**, *18*, 3659–3668.
- (17) (a) Kumar, A.; Pattarkine, M.; Bhadbade, M.; Mandale, A. B.; Ganesh, K. N.; Datar, S. S.; Dharmadhikari, C. V.; Sastry, M. *Adv. Mater.* **2001**, *13*, 341–344. (b) Nakao, H.; Shiigi, H.; Yamamoto, Y.; Tokonami, S.; Nagaoka, T.; Sugiyama, S.; Ohtani, T. *Nano Lett.* **2003**, *3*, 1391–1394. (c) Warner, M. G.; Hutchison, J. E. *Nat. Mater.* **2003**, *2*, 272–277.
- (18) (a) Dujardin, E.; Peet, C.; Stubbs, G.; Culver, J. N.; Mann, S. *Nano Lett.* **2003**, *3*, 413–417. (b) Fowler, C. E.; Shenton, W.; Stubbs, G.; Mann, S. *Adv. Mater.* **2001**, *13*, 1266–1269.
- (19) Li, Z.; Chung, S. W.; Nam, J. M.; Ginger, D. S.; Mirkin, C. A. *Angew. Chem., Int. Ed.* **2003**, *42*, 2306–2309.
- (20) He, Y. H.; Yuan, J. Y.; Shi, G. Q. *J. Mater. Chem.* **2005**, *15*, 859–862.
- (21) Johnson, B. J. S.; Wolf, J. H.; Zalusky, A. S.; Hillmyer, M. A. *Chem. Mater.* **2004**, *16*, 2909–2917.
- (22) (a) Berry, V.; Gole, A.; Kundu, S.; Murphy, C. J.; Saraf, R. F. *J. Am. Chem. Soc.* **2005**, *127*, 17600–17601. (b) Berry, V.; Rangaswamy, S.; Saraf, R. F. *Nano Lett.* **2004**, *4*, 939–942.
- (23) Berry, V.; Saraf, R. F. *Angew. Chem., Int. Ed.* **2005**, *44*, 6668–6673.
- (24) Turkevitch, J.; Stevenson, P. C.; Hillier, J. *J. Discuss. Faraday Soc.* **1951**, *11*, 55–75.
- (25) Hatchett, D. W.; White, H. S. *J. Phys. Chem.* **1996**, *100*, 9854–9859.
- (26) Vitanov, T.; Popov, A. *J. Electroanal. Chem.* **1983**, *159*, 437–446.
- (27) Ahrland, S.; Chatt, J.; Davies, N. R. *Q. Rev. Chem. Soc.* **1958**, *12*, 265–281.

- (28) Alcamo, I. E. *Fundamentals of Microbiology*, 5th ed.; Addison-Wesley Longman Inc.: Reading, MA, 1997.
- (29) Raimondi, F.; Scherer, G. G.; Kotz, R.; Wokaun, A. *Angew. Chem., Int. Ed.* **2005**, *44*, 2190–2209.
- (30) Morones, J. R.; Elechiguerra, J. L.; Camacho, A.; Holt, K.; Kouri, J. B.; Ramirez, J. T.; Yacaman, M. J. *Nanotechnology* **2005**, *16*, 2346–2353.
- (31) Davis, S. A.; Burkett, S. L.; Mendelson, N. H.; Mann, S. *Nature* **1997**, *385*, 420–423.
- (32) Mendelson, N. H. *Proc. Natl. Acad. Sci. U.S.A.* **1978**, *75*, 2478–2491.
- (33) Wakita, J.; Rafols, I.; Itoh, H.; Matsuyama, T.; Matsushita, M. *J. Phys. Soc. Jpn.* **1998**, *67*, 3630–3636.